JMEPEG (2011) 20:283–288
DOI: 10.1007/s11665-010-9663-8

1059-9495/$19.00

Synthesis and Multiferroic Properties of BFO Ceramics by Melt-Phase Sintering

M.S. Awan and A.S. Bhatti

(Submitted September 17, 2009; in revised form March 28, 2010)

Multiferroic ceramics ($Bi_{1.1}FeO_3$) were synthesized by the conventional powder metallurgy route by adopting the melt-phase sintering followed by rapid thermal quenching technique. Effect of sintering temperature on physical, structural, microstructural, electric, and magnetic properties was studied. X-ray diffraction and scanning electron microscopic studies showed that calcination and sintering promoted the desired perovskite ($BiFeO_3$) phase and density of the ceramics. Sintering temperature improved the bulk density of the samples as a result of this leakage current density decreased and electric polarization improved. Sample sintered at 850 °C showed bulk density up to 81%. Electric measurements showed spontaneous polarization, remnant polarization, and coercive field of 14.44 μC/cm^2, 5.47 μC/cm^2, and 25.50 kV/cm, respectively. Linear behavior of magnetization as a function of applied magnetic field confirms the antiferromagnetic nature of the $BiFeO_3$ compound at room temperature.

Keywords bulk density, leakage current, melt-phase sintering, multiferroic oxides, perovskite $BiFeO_3$, spontaneous polarization

1. Introduction

Multiferroics are the class of materials having coupled ferroelectric and ferro/antiferromagnetic order parameters that result in simultaneous ferroelectricity and magnetism in the single phase (Ref 1). These materials, therefore, not only have potential applications in magnetic and ferroelectric devices, but also the ability to couple the electric and the magnetic polarization in these materials, providing an additional degree of freedom in device design (Ref 2-6). This class of materials would offer a large application potential for new devices taking advantage of two coupled degrees of freedom based on local off-centered distortion and electron spin. The major applications of multiferroic materials are in spintronic devices, functional sensors, and multistate memory devices (Ref 3-6). Fundamental physics of these materials is also very interesting and fascinating besides the practical applications. The choice of such materials is very much limited due to inherent lack of simultaneous ferroelectric and ferromagnetic orders in a single phase at room temperature (RT).

The main multiferroic perovskite oxides studied so far include $BiFeO_3$, $BiMnO_3$, and $ReMnO_3$ (Re = Y, Ho-Lu). Among them, BFO bearing high Curie temperature ($T_C \sim 830$ °C) and a high Néel temperature ($T_N \sim 370$ °C) is technologically more desirable (Ref 7, 8). BFO has a rhombohedrally distorted perovskite crystal structure with space group *R*3*c* and G-type anti-ferromagnetism at RT (Ref 9). The ferroelectric mechanism in BFO is conditioned by the stereochemically active $6S^2$ lone pair of (Bi^{3+}) while the weak magnetic property is caused by residual moment from the canted (Fe^{3+}) spin structure (Ref 10). The magnetoelectric (ME) coupling effect between magnetic and electric behaviors occur through the lattice distortion of BFO when an electric field or a magnetic field is applied (Ref 6), which opened new avenues to the device design and application.

Though $BiFeO_3$ was discovered in the early 1960s and its structure and properties have been extensively studied (Ref 11, 12), transport measurements have been hampered by leakage problems. Low resistivity of the sample at RT makes the observation of the ferroelectric loop very difficult. This seriously limited the application of this material. In order to enhance the resistivity and observe a hysteresis loop, measurements were done at 80 K by Teague et al. (Ref 13). They obtained a ferroelectric hysteresis loop from a single crystal, with a spontaneous polarization of 3.5 μC/cm^2 in the (100) direction, but the saturation of the loop was not observed even at fields as high as 55 kV/cm. Latter, Wang et al. (Ref 14) and Pradhan et al. (Ref 15) adopted the rapid thermal sintering technique (RTST) and claimed the saturated ferroelectric loop at RT. They observed that spontaneous polarization, remnant polarization, and the coercive field were 8.9 μC/cm^2, 4.0 μC/cm^2, and 39 kV/cm, respectively; under an applied field of 100 kV/cm. They sintered the ceramic sample at 880 °C for 400 and 450 s. It was proposed that very high heating rate and short sintering time are beneficial for suppressing the leakage currents and to make it possible the measurement of ferroelectric loop at RT. Observation of saturated ferroelectric hysteresis loops in $BiFeO_3$ thin films at RT has been reported (Ref 7, 16). There are several reports (Ref 17, 18) on the fabrication of BFO dispersed in $BaTiO_3$ matrix to restrict the second phase, leakage current, and low resistivity in the sample. This enables the study of physical properties of $BiFeO_3$ rich phases. Other research work on $BiFeO_3$ ceramic involved synthesizing pure phase $BiFeO_3$ by leaching the impurity phase with dilute nitric

M.S. Awan and **A.S. Bhatti**, Center for Micro and Nano Devices, Department of Physics, COMSATS Institute of Information Technology, Park Road, Near Tramaree Chowk, Islamabad, Pakistan. Contact e-mail: sss_awan@yahoo.com.

acid (Ref 19), but the saturated loop was not obtained in this pure phase $BiFeO_3$ ceramic due to its lower density and high conductivity. For the investigation of electric properties and practical applications of $BiFeO_3$ ceramics, it is necessary and still a growing challenge to synthesize phase-pure and resistive samples. Liquid-phase sintering followed by rapid thermal quenching technique is improved processing technique used for the fabrication of BFO ceramics. However, detailed studies on microscopic grains, thermal, magnetic, and electrical properties related to frequency-dependent dielectric loss are still lacking in this potentially important ceramic.

In this paper, we report the synthesis and characterization of off-stoichiometric ($Bi_{1.1}FeO_3$) ceramics prepared by melt-phase sintering followed by rapid thermal quenching technique. Effect of sintering temperature on the structural, microstructural, electric polarization, and leakage current has been investigated. Samples revealed dense microstructures, pinched ferroelectric loops, and linear behavior of magnetization as a function of applied magnetic field at RT.

2. Experiment Details

Multiferroic ceramic of off-stoichiometric composition $Bi_{1.1}FeO_3$ were synthesis by the conventional powder metallurgy route adopting the melt-phase sintering followed by rapid thermal quenching technique. High-purity Bi_2O_3 (99.99%) and Fe_2O_3 (99.99%) powders were weighed in off-stoichiometric proportions (Bi:Fe = 1.1:1 mol ratio). Wet mixing technique was applied to achieve the homogeneous mixture of the starting materials. Acetone was used as the wetting medium. After thorough washing of the ball mill jar, raw powders, acetone, and ceramic balls were put into the ball mill and milling was carried out for 5 h. The powder to ball ratio was 1:10. After mixing the slurry was drawn into the petty dish and let it to dry in the fume hood over night. The next day, flake-like dried powder was ground and mixed with the help of motor and pester for more than 2 h. Mixed powder was then calcined at 725 °C for 60 min in air. After calcinations, the powder was again ground for 2 h in order to remove agglomerates formed during calcinations. Then, 3% PVA was added as the binding agent. The role of binder is to strengthen the green body and to keep contact among the powder particles. The binder added mixture was then uni-axially pressed (5 MPa) into the disk-like green compact with diameter (∅ = 15 mm) and thickness (T = 5 mm). Then, the prepared disk-like pellets were sintered by following the heat treatment cycle given in Fig. 1. Sintering temperature was optimized for which samples were sintered at four different temperatures, i.e., 775, 800, 825, and 850 °C. The sintering cycle includes five steps. In the first step, green compact was heated slowly from RT to 400 °C at the rate of 1 °C/min. The heating rate was kept very slow in order to remove the binder safely without cracking the pellet. In the second step, sample was kept at this temperature (400 °C) for 60 min for complete removal of the binder. In the third step, temperature was raised to 850 °C at a rate of 4 °C/min. In the fourth, isothermal step temperature was kept at 850 °C for 120 min. In this step, sintering of the green compact took place. Finally, the sample was air quenched by removing it from the heated furnace quickly. The idea was that melt-phase sintering followed by quenching may restrict the secondary phases in the sintered sample. This may help to improve the electrical

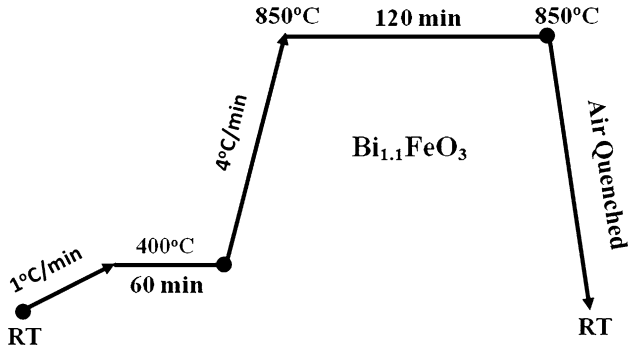

Fig. 1 Heat-treatment cycle for sintering of $BiFeO_3$ ceramic samples

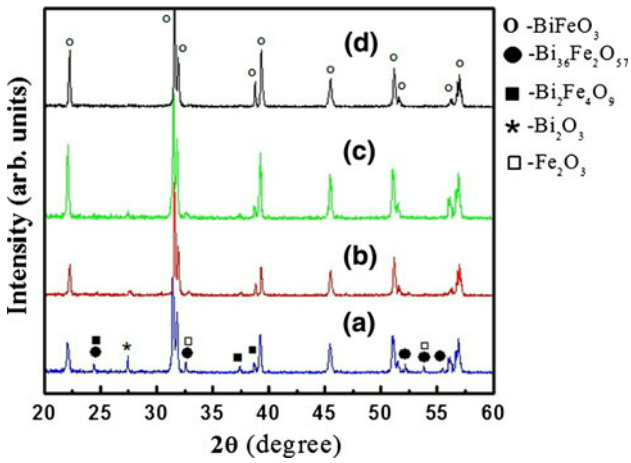

Fig. 2 XRD patterns of the $BiFeO_3$ ceramic samples sintered at (a) 775 °C, (b) 800 °C, (c) 825 °C, and (d) 850 °C. All the samples were sintered for 120 min in air and air quenched

properties as secondary phases may cause leakage currents. Actually, there may not be sufficient time during quenching for impurity/second phases to be stable.

For electrical measurements, the samples were prepared to have a clean and smooth surface for electrodes. With the help of diamond cutter, pellets were cut into slices of thickness ~4-5 mm. Later these slices were further thinned down to 1.5 mm thickness by grinding on the silicon carbide sand paper. Finally, samples were polished with the help of diamond paste and then dried with the compressed air to remove the contamination. These neat and clean surfaces were used for electrode connections for electrical measurements. Silver (Ag) paste electrodes with a 1.5-mm diameter were pasted on both sides of the samples. Ferroelectric properties of the $BiFeO_3$ ceramics were measured using a RT6000 ferroelectric tester under virtual ground conditions. Magnetic properties were measured using vibrating sample magnetometer (VSM). SEM was used to study the surface morphology of the fractured ceramics. All the measurements were carried out at RT.

3. Results and Discussion

Figure 2 presents the x-ray diffraction (XRD) patterns of the $BiFeO_3$ ceramic samples prepared by melt-phase sintering

followed by rapid thermal quenching techniques. Samples were characterized by XRD studies between the 2θ-scan regions of (20°-60°). BFO samples were sintered at four different temperatures, i.e., 775, 800, 825, and 850 °C. All the samples were sintered for 120 min and then air quenched. The phase analysis was performed by considering the hexagonal BFO unit cell. The hexagonal unit cell of BFO system contains two formula pseudocubic units (distorted cubic) cells of $BiFeO_3$. The lattice parameters for hexagonal unit cell of $BiFeO_3$ were calculated by using the XRD software named "CELL." The indexed XRD pattern for BFO sample sintered at 850 °C is shown in Fig. 3. The (*hkl*) planes in the XRD pattern for BFO were indexed by comparing them with the data of JCPD card of PDF # 71-2494. Using 2θ values from the XRD graph and (*hkl*) values from the standard JCPD card the lattice parameters for the hexagonal unit cell were generated. The calculated values of lattice parameters for the sample sintered at 850 °C are given as a = 5.58(1) Å and c = 13.87(4) Å. The reported lattice parameters for the BFO hexagonal unit cell are a = 5.58(1) Å and c = 13.86(2) Å. The calculated values of the lattice parameters for the hexagonal unit cell of $BiFeO_3$ matched well with the values reported in the literature. The major reflection was from the (110) peak which appeared at (2θ = 31.49°). All other BFO peaks were marked and identified by comparison. Sintering temperature does not show any significant effect on the lattice parameters. For low temperature sintering (775 °C) some additional peaks appeared in the XRD graph like at (2θ = 27.43° and 32.61°) are the reflections from unreacted Bi_2O_3 and Fe_2O_3 powders, respectively. Some nonperovskite impurity phases such as $Bi_2Fe_4O_9$ and $Bi_{36}Fe_2O_{57}$ were also identified. The presence of these unreacted powders and impurity phases may be attributed to the use of unsuitable sintering conditions. One other reason may be that Bi_2O_3 is not fully liquefied under these sintering conditions as its melting point is (~817 °C). In other parts of the samples, the remaining liquefied Bi_2O_3 may be insufficient to form $BiFeO_3$ phase, resulting in unreacted powders (Bi_2O_3, Fe_2O_3) and impurity phases as shown in Fig. 2(a). We kept the sintering time constant and vary the sintering temperature. Later the samples prepared under the identical conditions were sintered at 800, 825 and 850 °C for 120 min. On increasing the sintering temperature, the peaks due to unreacted powders (Bi_2O_3 and Fe_2O_3) were reduced and also other impurity phases were eliminated to some extent as shown in Fig. 2(b-d). The XRD pattern in Fig. 2(d) can be indexed only for perovskite BFO phase. It is believed that at sintering temperature the low melting point (Bi_2O_3) powder converts into the liquid phase. This (Bi_2O_3) liquid wet the (Fe_2O_3) powder particles. As a result, (Bi_2O_3) reacts with (Fe_2O_3) powder particles to form the desired ($BiFeO_3$) phase. We obtained phase-pure BFO ceramic sample with a little additional peak from (Bi_2O_3) for the sintering temperature of 850 °C as shown in Fig. 2(d). This additional peak may be due to the use of excess (Bi_2O_3) powder in the starting material. Similar kind of behavior is also observed by some other researchers (Ref 14, 20, 21).

The impurity phases appeared in the sample prepared by melt-phase sintering and rapid thermal quenching techniques at 825 °C may be attributed to the fact that this sintering temperature is very close to the melting point of the Bi_2O_3 (~817 °C). During sintering at 825 °C, the melting of Bi_2O_3 was probably not complete. Therefore, the liquid Bi_2O_3 is insufficient to wet the whole Fe_2O_3 particles and it is not possible to complete the solid-state reaction between the powders. As a result we observed some additional peaks along with the main $BiFeO_3$ peaks. This can be seen in Fig. 2(c). As the mixture powder was calcined prior to sintering, XRD patterns in Fig. 4 give the phase development in the sintered and calcined material. For comparison, the XRD pattern of the powder mixture of well-mixed raw materials is also presented as shown in Fig. 4(a). After calcination, the powder is not completely converted into $BiFeO_3$ phase. It is noted that the sintering temperature less than 850 °C is not sufficient for sintering of BFO samples. Sintering at lower temperatures resulted in the formation of undesirable phases which ultimately affected the ferroelectric properties.

Figure 5 shows the magnetization of the BFO ceramic sample as a function of applied magnetic field. The measurement was carried out on the ceramic sample sintered at 850 °C for 120 min at RT. It is evident that magnetization is a linear function of applied magnetic field. This behavior is typical of antiferromagnetic materials (Ref 22). On the other hand, the

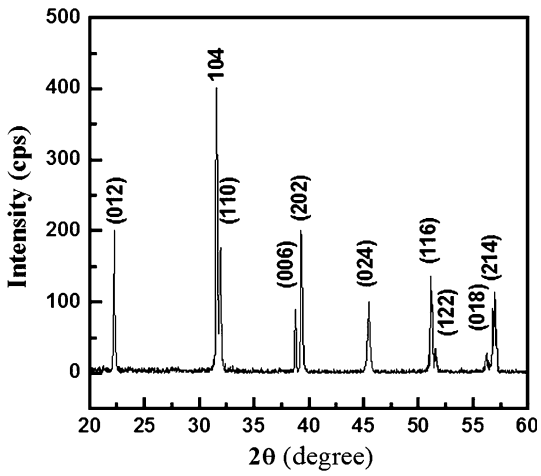

Fig. 3 Indexed XRD pattern of the $BiFeO_3$ ceramic sample sintered at 850 °C for 120 min in air, where index (*hkl*) is based on the hexagonal crystal structure (JCPD card-PDF # 71-2494)

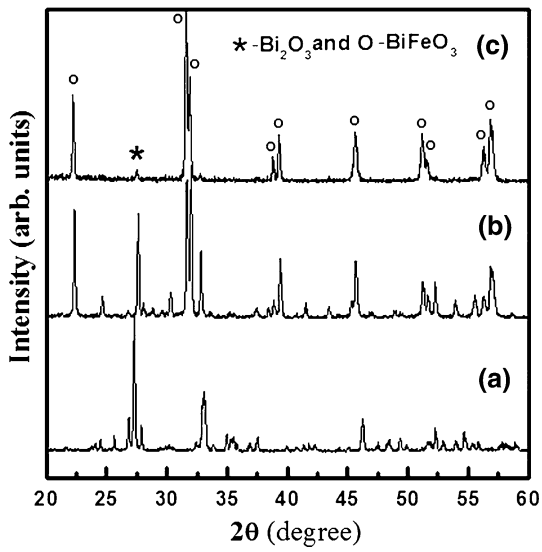

Fig. 4 XRD patterns of the (a) powder mixture of Bi_2O_3 and Fe_2O_3, (b) powder calcined at 725 °C for 60 min, and (c) $BiFeO_3$ ceramic sample sintered at 850 °C for 120 min in air

magnetization and magnetic hysteresis results confirm the absence of canted ferromagnetic behavior in this sample. This suggests the absence of Fe-related clusters or impurities in the sample. Surface morphology of the sintered ceramic samples was investigated by the SEM studies. Figure 6(a-d) is the SEM micrographs of the samples sintered at 775, 800, 825, and 850 °C for 120 min, respectively. Micrographs were taken from the fractured surfaces of the samples. It is evident from the SEM micrographs that they consist of mixed cores and fine particles. The effect of sintering temperature is evident from the micrographs in the form of diffusion of the particles. The microstructure of the sample sintered at 850 °C is relatively dense. Small and big particles are well connected to each other. Less porosity, smooth surface, and well-connected grains are essential for the good ferroelectric properties.

During sintering diffusion of particles may take place which results in bigger particles and necking between the particles as shown by SEM micrographs in Fig. 6. The empty space between the particles is reduced and hence bulk density of the ceramic sample improves. Furthermore, the existence of liquid phase during the sintering process will also be beneficial to increase the bulk density of the sintered ceramic samples. During sintering process increase in the bulk density was observed. Figure 7 is the graph between the relative bulk

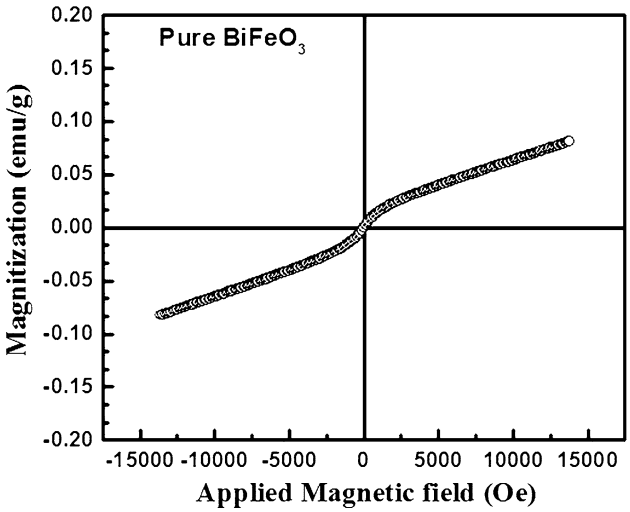

Fig. 5 Magnetization behavior of $BiFeO_3$ ceramic sample (sintered at 850 °C) as a function of applied magnetic field

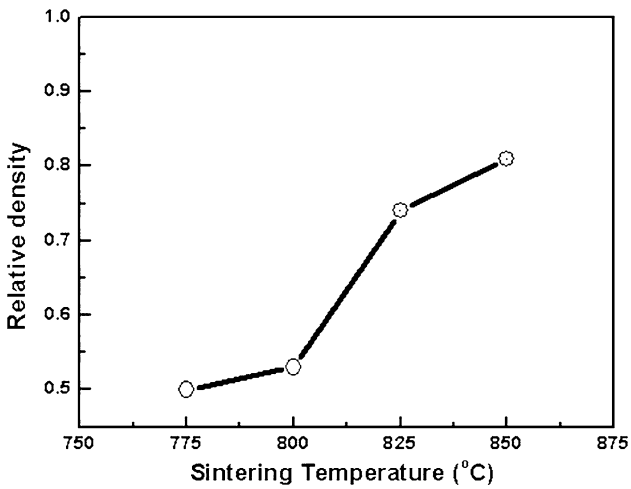

Fig. 7 Relative bulk densities of $BiFeO_3$ ceramics sintered at different temperatures

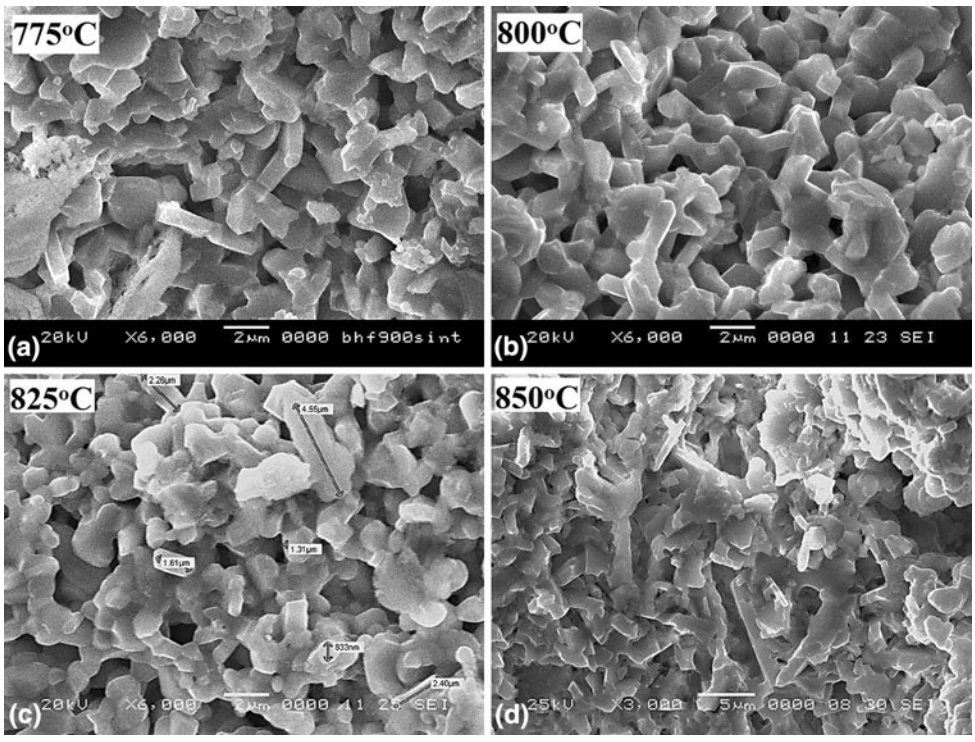

Fig. 6 SEM micrographs of the $BiFeO_3$ ceramic samples sintered at (a) 775 °C, (b) 800 °C, (c) 825 °C, and (d) 850 °C

densities of the sintered $BiFeO_3$ ceramic samples at different temperatures. The density was measured by Archimedes method. The graph shows a rapid increase in the bulk density from 53% to 74% during sintering between the temperatures 800 and 825 °C. It should be noted that this change in apparent bulk density is just across the melting point of Bi_2O_3, which is ~817 °C. A relative density of 81% was observed when the samples were sintered at 850 °C, indicating that compact ceramic could be synthesized using this technique. Porosity and density significantly affect the ferroelectric properties.

Ferroelectric properties were conducted by measuring polarization (P-E) hysteresis loops of the ceramic samples. Figure 8 is the P-E loops of the BFO samples sintered at 775, 800, 825, and 850 °C. The measurements were carried out for an applied field of 80 kV/cm. Sample sintered at 775 °C showed a pinched P-E loop with very low ferroelectric properties. This may be due to the porous microstructure and presence of impurity/secondary phases as indicated by the XRD results. Sample sintered at 850 °C was phase pure and showed a slim and loose P-E loop with the spontaneous polarization, remnant polarization, and coercive field are 14.44 μC/cm^2, 5.47 μC/cm^2, and 25.50 kV/cm, respectively. Figure 9 shows

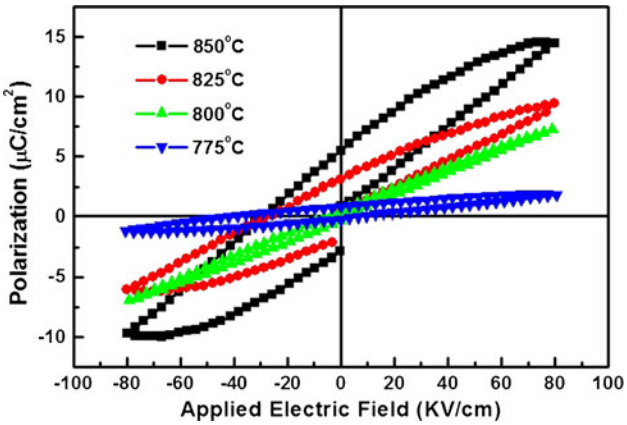

Fig. 8 Polarization (P-E) hysteresis loops of $BiFeO_3$ ceramics sintered at (a) 775 °C, (b) 800 °C, (c) 825 °C, and (d) 850 °C

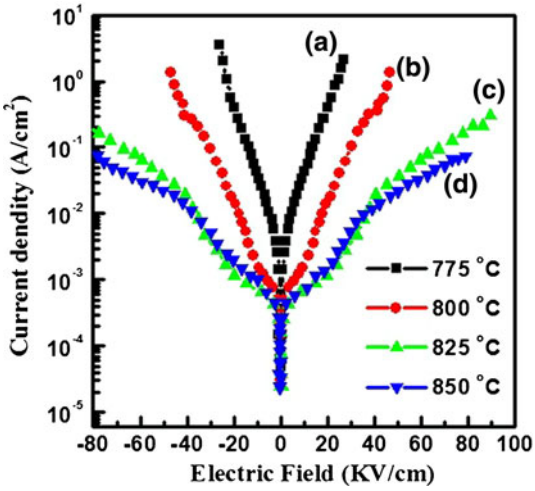

Fig. 9 Leakage current as a function of applied electric field for the samples sintered at (a) 775 °C, (b) 800 °C, (c) 825 °C, and (d) 850 °C

the leakage current density as a function of applied electric field for the samples sintered at different temperatures. Current density decreases with increasing the sintering temperature. High-leakage currents in the sample sintered at low temperature may be due to the porosity and presence of the impurity phases as indicated in SEM micrographs (Fig. 6a) and XRD results (Fig. 2a). These results are in agreement with the results obtained by others (Ref 23). It is known that the deviation from oxygen stoichiometry (non-perovskite phases) leads to valence fluctuation of Fe ions from +3 to +2 state in $BiFeO_3$, resulting in high conductivity (Ref 16). Our explanation for the resistive off-stoichiometric $BiFeO_3$ ceramic samples synthesized by the melt-phase sintering and rapid thermal quenching technique is that excess Bi_2O_3 will cover the Bi loss caused due to its evaporation. This will maintain the required stoichiometry of the BFO compound. On the other hand, rapid thermal quenching may reduce the formation of undesired phases.

4. Conclusion

In conclusion, a phase-pure $BiFeO_3$ ceramic was synthesized adopting the melt-phase sintering followed by rapid thermal quenching technique. Calcination promoted the desired perovskite ($BiFeO_3$) phase in the powder mixture. Sintering temperature affected the physical, microstructural, and electric properties of the ceramics. An increase in sintering temperature improved bulk density of samples; as a result of this, leakage current density decreased and polarization improved. Sample sintered at 850 °C showed bulk density up to 81% and remnant polarization of 5.47 μC/cm^2. Magnetic measurements showed that ceramic $BiFeO_3$ is antiferromagnetic at RT.

References

1. J.F. Scott, Data Storage: Multiferroic Memories, *Nat. Mater.*, 2007, **6**, p 256–257
2. W. Eerenstein, N.D. Mathur, and J.F. Scott, Multiferroic and Magnetoelectric Materials, *Nature*, 2006, **442**, p 759–765
3. T. Kimura, T. Goto, H. Shintani, K. Ishizaka, T. Arima, and Y. Tokura, Magnetic Control of Ferroelectric Polarization, *Nature*, 2003, **426**, p 55–58
4. S. Dong, J.F. Li, and D. Viehland, Ultrahigh Magnetic Field Sensitivity in Laminates of TERFENOL-D and $Pb(Mg_{1/3}\ Nb_{2/3})O_3$-$PbTiO_3$ Crystals, *Appl. Phys. Lett.*, 2003, **83**, p 2265–2267
5. S. Dong, Magnetoelectric Gyration Effect in $Tb_{1-x}Dy_xFe_{2-y}$/Pb(Zr, Ti)O_3 Laminated Composites at the Electromechanical Resonance, *Appl. Phys. Lett.*, 2006, **89**(24), p 243512–243513
6. S.-W. Cheong and M. Mostovoy, A Magnetic Twist for Ferroelectricity, *Nat. Mater.*, 2007, **6**, p 13–20
7. J. Wang, J.B. Neaton, H. Zheng, V. Nagarajan, S.B. Ogale, B. Liu, D. Viehland, V. Vaithyanathan, D.G. Schlom, U.V. Waghmare, N.A. Spaldin, K.M. Rabe, M. Wuttig, and R. Ramesh, Epitaxial $BiFeO_3$ Multiferroic Thin Film Heterostructures, *Science*, 2003, **299**, p 1719–1722
8. J.B. Neaton, C. Ederer, U.V. Waghmare, N.A. Spaldin, and K.M. Rabe, First-Principles Study of Spontaneous Polarization in Multiferroic $BiFeO_3$, *Phys. Rev.*, 2005, **71**, p 014113
9. G.A. Smolenskii and I. Chupis, Ferroelectromagnets, *Sov. Phys. Usp.*, 1982, **25**, p 475
10. P. Fischer, M. Polomska, I. Sosnowska, and M. Szymanski, Temperature Dependence of the Crystal and Magnetic Structures of $BiFeO_3$, *J. Phys. C: Solid State Phys.*, 1980, **13**(10), p 1931

11. J.D. Bucci, B.K. Robertson, and W.J. James, The Precision Determination of the Lattice Parameters and the Coefficients of Thermal Expansion of $BiFeO_3$, *J. Appl. Cryst.*, 1972, **5**, p 187–191
12. F. Kubel and H. Schmid, Structure of a Ferroelectric and Ferroelastic Monodomain Crystal of the Perovskite $BiFeO_3$, *Acta Crystall. B*, 1990, **46**, p 698–702
13. J.R. Teague, R. Gerson, and W.J. James, Dielectric Hysteresis in Single Crystal $BiFeO_3$, *Solid State Commun.*, 1970, **8**(13), p 1073–1074
14. Y.P. Wang, L. Zhou, M.F. Zhang, X.Y. Chen, J.M. Liu, and Z.G. Liu, Room-Temperature Saturated Ferroelectric Polarization in $BiFeO_3$ Ceramics Synthesized by Rapid Liquid Phase Sintering, *Appl. Phys. Lett.*, 2004, **84**(10), p 1731–1733
15. A.K. Pradhan, K. Zhang, D. Hunter, J.B. Dadson, G.B. Loutts, P. Bhattacharya, R. Katiyar, J. Zhang, D.J. Sellmyer, U.N. Roy, Y. Cui, and A. Burger, Magnetic and Electrical Properties of Single-Phase Multiferroic $BiFeO_3$, *J. Appl. Phys.*, 2005, **97**, p 093903
16. V.R. Palkar, J. John, and R. Pinto, Observation of Saturated Polarization and Dielectric Anomaly in Magnetoelectric $BiFeO_3$ Thin Films, *Appl. Phys. Lett.*, 2002, **80**, p 1628–1630
17. K. Ueda, H. Tabata, and T. Kawai, Coexistence of Ferroelectricity and Ferromagnetism in $BiFeO_3$-$BaTiO_3$ Thin Films at Room Temperature, *Appl. Phys. Lett.*, 1999, **75**, p 555
18. M. Mahesh Kumar, A. Srinivas, and S.V. Suryanarayan, Structure Property Relations in $BiFeO_3$/$BaTiO_3$ Solid Solutions, *J. Appl. Phys.*, 2000, **87**, p 855
19. M. Mahesh Kumar, V.R. Palkar, K. Srinivas, and S.V. Suryanarayana, Ferroelectricity in a Pure $BiFeO_3$ Ceramic, *Appl. Phys. Lett.*, 2000, **76**(19), p 2764–2766
20. V. Fruth, L. Mitoseriu, D. Berger, A. Ianculescu, C. Matei, S. Preda, and M. Zaharescu, Preparation and Characterization of $BiFeO_3$ Ceramic, *Solid State Chem.*, 2007, **35**, p 193–202
21. I. Sosnowska, T.P. Neumaier, and E. Steichele, Spiral Magnetic Ordering in Bismuth Ferrite, *J. Phys C*, 1982, **15**(23), p 4835
22. V.R. Palkar, C. Darshan Kundaliya, S.K. Malik, and S. Bhattacharya, Magnetoelectricity at Room Temperature in $Bi_{0.9-x}Tb_xLa_{0.1}FeO_3$ System, *Phys. Rev. B*, 2004, **69**, p 212102
23. S.-T. Zhang, L.-H. Pang, Y. Zhang, M.-H. Lu, and Y.-F. Chen, Preparation, Structures, and Multiferroic Properties of Single Phase $Bi_{1-x}La_xFeO_3$ (x = 0-0.40) Ceramics, *J. Appl. Phys.*, 2006, **100**(11), p 114108